

# HIGH-RESOLUTION OBSERVATIONS OF THE CO GAS SURROUNDING THE CORE OF CRL 618

ARSEN R. HAJIAN,<sup>1,2</sup> J. A. PHILLIPS,<sup>3</sup> AND YERVANT TERZIAN<sup>1</sup>

*Received 1995 June 21; accepted 1996 February 20*

## ABSTRACT

Recently acquired CO(1–0) observations at 115 GHz with the Owens Valley Radio Observatory have revealed the presence of previously undetected material surrounding CRL 618. The observations have a beam size of  $2''.0 \times 1''.6$  and are more sensitive than any interferometric observations of the source thus far. Our maps reveal the presence of a circular emission region with a radius of  $\approx 15''$  surrounding the core of CRL 618. It is probable that this halo structure is a shell of ejecta from the progenitor of CRL 618, which underwent a period of significant mass loss while ascending the asymptotic giant branch. The CO halo is clumpy and surrounds the bright molecular core of CRL 618, possibly shaping the core's weak bipolar appearance. As in the case of the CS line we have previously observed, the spectral profile of the CO line is similar to a P Cygni feature. The morphology of the absorption feature is that of a point source centered close to, but not coincident with the H II position. In addition, we have imaged the high-velocity outflow from the core, and we find that the redshifted and blueshifted emission comes from point sources that are distinctly separated, with the redshifted lobe west of the blueshifted lobe.

*Subject headings:* ISM: individual (CRL 618) — ISM: jets and outflows — radio lines: ISM — stars: AGB and post-AGB

## 1. INTRODUCTION

CRL 618 is a fruitful observational source, with several interesting spectral and spatial characteristics. A proto-planetary nebula (PPN) in the short-lived (and thus rare) transition phase from red giant to planetary nebula, CRL 618 exhibits signatures across the spectrum from numerous astrophysical processes. Surrounding the central star is an optically thick and dusty core that reflects the stellar spectrum along its bipolar lobes (Westbrook et al. 1975). The core is brightening on timescales of a half-century (Gottlieb & Liller 1976). The optical and IR spectrum of the core also emits a nebular line spectrum dominated by emission from atomic gas (Trammell, Dinerstein, & Goodrich 1993; Schmidt & Cohen 1981; Kelly, Latter, & Rieke 1992). At radio wavelengths, the source has been seen to brighten on timescales of 3 yr: the flux density of free-free photons is increasing as the H II region expands and ionizes more and more gas (Kwok & Feldman 1981; Kwok & Bignell 1984). Thermal emission from dust is responsible for a strong continuum at infrared, millimeter, and submillimeter wavelengths (Westbrook et al. 1975; Sopka et al. 1985; Kwok, Hrivnak, & Milone 1986), upon which is superposed a rich assortment of spectral emission lines from a variety of molecular species.

Although numerous, most of the existing observations of molecules in CRL 618 have been conducted with large single-dish telescopes. In these cases, detecting the molecular emission is facilitated by the large collecting areas of the solitary dishes, but little or no spatial information is afforded by beam sizes of  $10''$ – $1'$ . Currently single-dish observations include lines of CO, HCN, SiO, C<sub>2</sub>O, C<sub>3</sub>N, and

HCO<sup>+</sup> (Lo & Bechis 1976; Bujarrabal et al. 1988; Bachiller et al. 1988; Cernicharo et al. 1989; Martin-Pintado & Bachiller 1992; Deguchi, Claussen, & Goldsmith 1986). The line profiles are usually parabolic, but some lines appear as P Cygni features.

The arrival of interferometry at millimeter wavelengths has afforded a new approach. With beam sizes of a few arcseconds, it is now possible to resolve the spatial morphology of CRL 618 and to provide a better understanding of the evolution, structure, and origin of the star and the surrounding ejecta. There are currently only a handful of published synthetic aperture millimeter observations of CRL 618: they include HCN by Neri et al. (1992), <sup>12</sup>CO by Shibata et al. (1993), <sup>13</sup>CO by Yamamura et al. (1994), and CS by Hajian, Phillips, & Terzian (1995). These studies achieved synthesized beams of  $\approx 3''$ – $5''$ .

CRL 618 is comprised of various components, including a tiny  $\sim 3''$  core, a slightly E–W elongated core outflow that is  $\approx 9''$  in size, a spherical halo extending at least  $16''$  in diameter, and an unresolved high velocity outflow consisting of two offset point sources. Different molecules are useful for probing each of these components. HCN and CS are tracers of high-density gas. The HCN observations of Neri et al. (1992) and the CS observations by Hajian et al. (1995) imaged the  $\sim 5''$  core of CRL 618, showing an essentially spherical distribution with some protrusions in the diagonal directions. Both lines have strong P Cygni absorption features, and both lines showed nonspherical redshifted and blueshifted emission with displaced emission centers, conditions indicative of a bipolar outflow. A recent 23 GHz continuum study performed at the VLA, which achieved  $\approx 0''.1$  resolution (Martin-Pintado et al. 1995), shows a disk of material  $\approx 1''$ . Trailing wisps and filaments of NH<sub>3</sub> were also detected, probably the result of the wind from the central star impinging on the inner surface of the (collimating) disk. The CO maps by Shibata et al. (1993) and Yamamura et al. (1994) trace the weakly bipolar core outflow. These spectra show parabolic line profiles with no significant blueshifted absorption, and the images show a

<sup>1</sup> Department of Astronomy and NAIC, Cornell University, Ithaca, NY 14853.

<sup>2</sup> United States Naval Observatory, USNO/NRL Optical Interferometer Project, 3450 Massachusetts Avenue NW, Washington, DC 20392-5420.

<sup>3</sup> Owens Valley Radio Observatory, Caltech 105-24, Pasadena, CA 91125.

featureless, approximately spherical structure comprising the CO outflow. Both studies concluded that, with the exception of the red wing of the high-velocity outflow detected by Shibata et al. (1993), there is no significant deviation from spherical symmetry in the CO halo outflow.

Until now, previous observations have not had the combination of angular resolution and sensitivity required to detect the totality of the CO structure surrounding CRL 618. In this paper, we present new observations of the 115 GHz CO (1–0) transition from CRL 618, conducted at Owens Valley Radio Observatory (OVRO). With the addition of a sixth antenna, the OVRO system is sensitive enough to detect previously unseen CO emission, and it provides enough coverage in the UV plane to see a detailed image of the circumstellar environment. Our goals are (1) to use the extra sensitivity to probe any faint halo surrounding CRL 618, and (2) to use the small synthesized beam to search for localized structures that may hint at the nature of the mechanisms sculpting the molecular nebula.

We present our observing strategy in § 2, followed by the results in § 3, and a summary of the conclusions in § 4.

## 2. OBSERVATIONS

We initially observed the CO(1–0) line and the 2.6 mm continuum of CRL 618 using the millimeter interferometer of the OVRO during 1994 March 1, 1995 January 22, and 1995 January 27. The first of these observations was performed with the five-element array, and the latter two sessions were performed with the upgraded six-element interferometer. The total integration time for CRL 618 was 25 hr, and the average single sideband system temperature was approximately 900 K for all three observations. The phase center of the map was located at  $\alpha = 04^{\text{h}}39^{\text{m}}34^{\text{s}}.0$ ,  $\delta = +36^{\circ}01'16''$  (epoch 1950.0).

We obtained CO spectra using a high-speed digital correlator (Padin et al. 1993). A 128 MHz band with 256 independent frequency channels was centered on the CO(1–0) transition frequency at 115.27 GHz and Doppler shifted to LSR velocity of  $-25 \text{ km s}^{-1}$ . The observations of CRL 618 were interleaved every 30 minutes with the nearby point source 3C 84 in order to monitor the phase behavior of the array. We used 3C 84 and 3C 273 to calibrate the bandpass response of the system. The absolute flux scale was determined from observations of the planet Neptune.

We calibrated the data using the Caltech “mma” software package (Scoville et al. 1993) and imaged the nebula using AIPS. Uniform weighting of the visibility data gave a  $2''.0 \times 1''.6$  CLEAN beam at position angle  $-88^\circ.66$ . The maps presented in this paper have not been corrected for the  $\approx 1'$  FWHM response of the primary beam. With the recent addition of a sixth antenna to the OVRO array, we were able to calibrate the data using an antenna-based algorithm that measures and corrects phase closure errors. The data were self-calibrated and mapped using a combination of AIPS and DIFMAP routines. The resulting  $3 \sigma$  noise level per  $1.3 \text{ km s}^{-1}$  channel is  $291 \text{ MJy beam}^{-1}$ .

## 3. RESULTS

### 3.1. 2.6 mm Continuum

In order to extract the continuum spectrum from the position-velocity data, we averaged 70 channels on both edges of the spectrometer bandpass. The channels in the edges of both bands showed a point source that was unre-

solved by our synthesized beam and that was centered within  $1''.0$  of the continuum emission from the H II region detected at longer radio wavelengths (Kwok & Bignell 1984). The continuum flux density we have detected is  $2.07 \text{ Jy}$ . We do not think that this is significantly higher than the  $1.48 \text{ Jy}$  detected at 118 GHz by Shibata et al. (1993) given the absolute flux calibration problems inherent to millimeter interferometry.

### 3.2. CO(1–0) Low-Velocity Line Emission

After subtracting the CLEAN components of the continuum point source from the observed data, we CLEANed each channel separately. The grand CO spectrum is displayed in Figure 1. We chose the velocity scale with respect to the  $-21.5 \text{ km s}^{-1}$  systemic velocity of CRL 618, and we computed the spectrum by integrating the total flux within the central  $\pm 20''$  of the map. Note the absorption feature that is apparent blueward of the emission line at about the  $10 \sigma$  level. The overall line profile looks like a P Cygni feature, which is characteristic of optically thick outflowing stellar envelopes. It is possible that the absorption feature is comprised of two distinct components (one broad and another narrow), but the data do not make this conclusion definite. Similar absorption features have been seen in lines of CS(2–1) (Hajian et al. 1995), CO(3–2) (Gammie et al. 1989), CO(2–1), HCN, and NH<sub>3</sub> (Cernicharo et al. 1989), and in several molecules comprising the winds of CRL 2688 (Young et al. 1992; Kawabe et al. 1987). Our detection in Figure 1 of the absorption feature from CO(1–0) can now be included as well. It is currently believed that the absorption feature is caused by the emitting low-velocity wind we have detected being absorbed by a medium-velocity outflow situated between the observer and the central star. Emission from the medium-velocity outflow has been seen with single-dish telescopes and not in interferometric observations, indicating that the low-velocity outflow region is smaller and thus located inside the medium-velocity outflow. As in the case of the CS (Hajian et al. 1995) and HCO<sup>+</sup> (Cernicharo et al. 1989), the CO(1–0) line exhibits absorption below the continuum (i.e., the line flux is negative), which suggests that the medium-velocity gas is

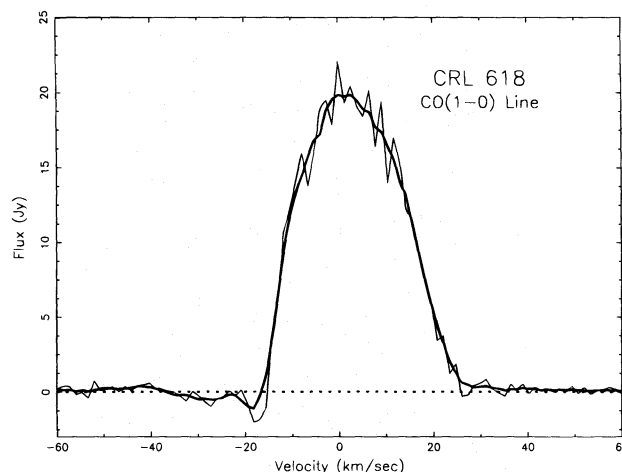


FIG. 1.—Raw CO(1–0) line spectrum as a function of velocity is shown with a thin line. The thick line is a heavily smoothed version of the raw data. The spectral resolution is  $1.3 \text{ km s}^{-1} \text{ channel}^{-1}$ . The continuum flux of  $2.07 \text{ Jy}$  has been subtracted, and the systemic velocity of  $-21.5 \text{ km s}^{-1}$  has been removed. We have detected significant absorption blueward of the emission line.

thick enough to intercept and absorb continuum radiation as well as emitted line radiation. Since the minimum in the absorption feature is approximately 2.03 Jy below the 2.07 Jy continuum, the medium-velocity outflow is very thick and has an optical depth that is about  $\approx 4$ .

The velocity maps near the line peak are shown in Figure 2 for the velocity range  $-19.4 < v < +20.7 \text{ km s}^{-1}$  with a resolution of  $1.3 \text{ km s}^{-1}$ . Considerable structure is present. Notice the localized blobs in the halo of CRL 618. While some of the blobs are only present in one velocity panel, many of them are intense ( $5 \sigma$  or higher) and exist over several velocity channels. This is the first sighting of clumpy structure within the shell of CRL 618.

In order to consider the totality of the detected CO gas, we averaged all of the line flux for  $-35 < v < +35 \text{ km s}^{-1}$ . This is displayed in Figure 3. The overall appearance of the nebula suggests a double-envelope morphology: an inner envelope (i.e., the core outflow) that has a mildly elongated appearance, and an outer envelope (i.e., the halo) that is spherical. Our observations show that the core distribution can be fitted by an ellipse with the major axis in the E-W direction and with an axial ratio of 0.76. Several of the localized CO concentrations existing in Figure 2 are apparent at a higher level in Figure 3.

The agreement between our observations and those of Shibata et al. (1993) is very good. Our noise level is more

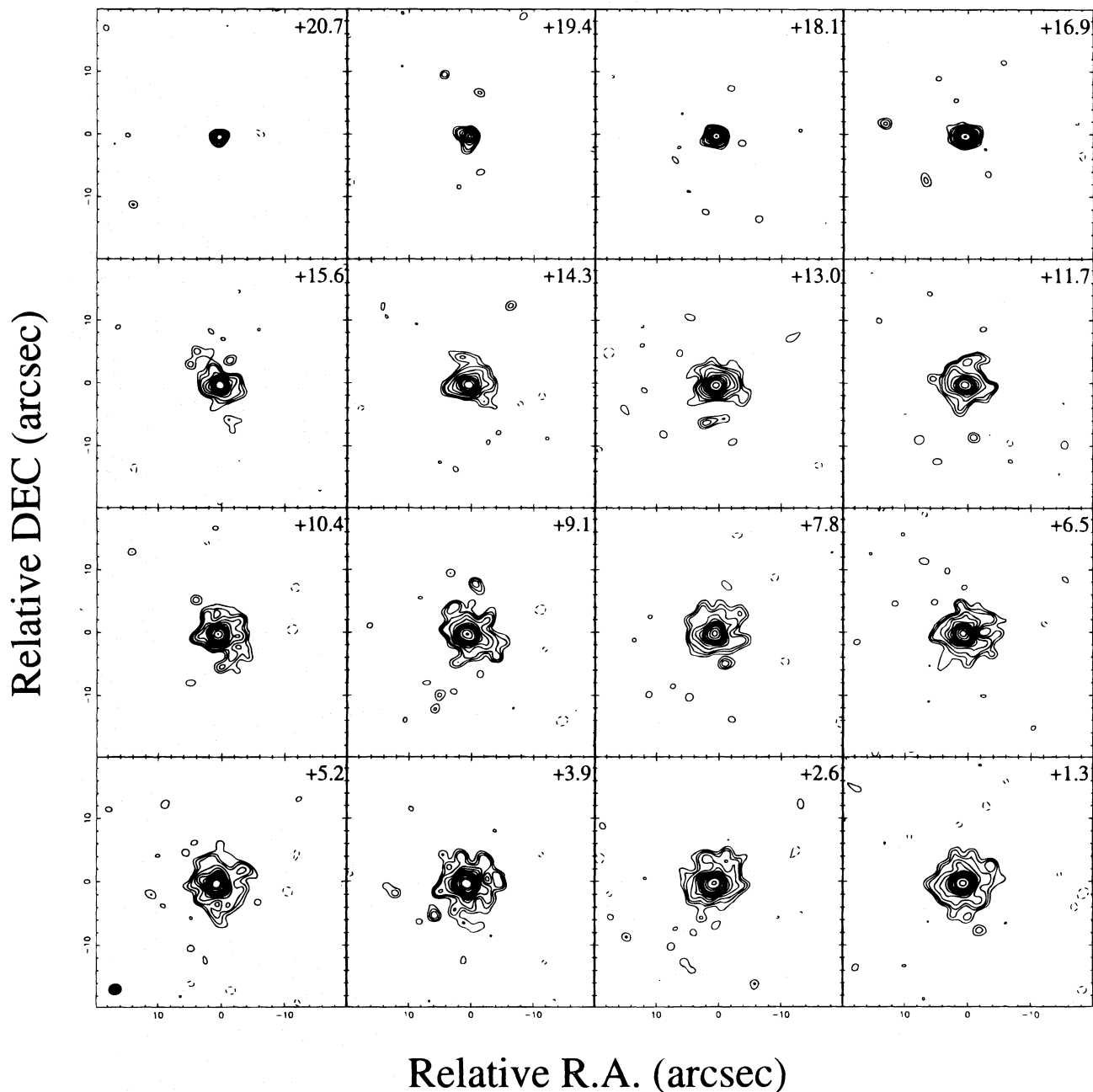


FIG. 2.—CO(1–0) line emission over the velocity range, defined by the parabolic emission line. The spectral resolution is  $1.3 \text{ km s}^{-1} \text{ channel}^{-1}$ . Velocities, listed in the upper right-hand corner of each map, are in  $\text{km s}^{-1}$  and are the channel central velocity with respect to the systemic velocity of  $-21.5 \text{ km s}^{-1}$ . The continuum flux of 2.07 Jy has been subtracted. Note the absorption detected in the channels blueward of the line center. The contour levels are at the  $-10, -8, -6, -4, -3, 3, 4, 5, 7, 9, 11, 13, 15, 17, 20, 25, 30, 40, 50$ , and  $60 \sigma$  levels, where the  $2 \sigma$  level is  $197 \text{ mJy beam}^{-1} \text{ channel}^{-1}$ . The synthesized beam is  $2''.0 \times 1''.6$  and is shown in the lower left-hand corner.

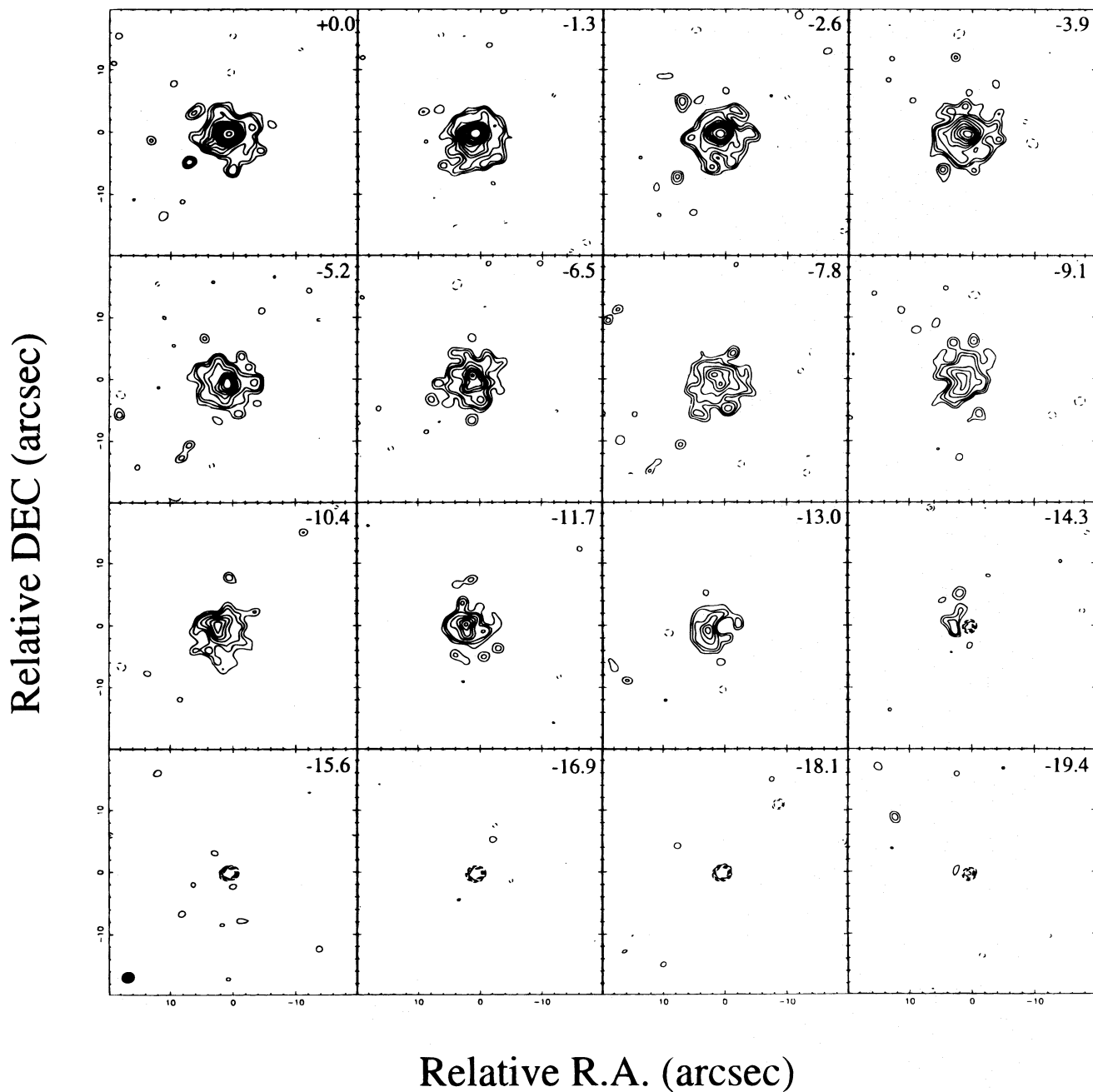


FIG. 2—Continued

than 3 times smaller, and since the surface brightness of the halo and the blueshifted absorption feature are mostly between the 3 and 9  $\sigma$  levels in our map, they would not have been detected in the observations by Shibata et al. (1993). Furthermore, assuming that the blobs and the absorption feature are unresolved, our observations have the advantage of a beam area that is about 4 times smaller, diminishing the effects of beam dilution.

### 3.3. CO(1–10) High-Velocity Line Emission

Upon careful consideration of the spectrum for high-velocity channels, it became clear to us that there was some low-intensity emission present. In order to accrue enough signal to make an image, we integrated detected emission from  $+35 < v < +65$   $\text{k s}^{-1}$  for the red wing and from

$-65 < v < -35$   $\text{k s}^{-1}$  for the blue wing. Unfortunately, with our chosen method of continuum subtraction, we must sacrifice information regarding the high-velocity outflow for  $|v| > 65$   $\text{k s}^{-1}$  in order to achieve an accurate continuum measurement. In each map, the  $2\sigma$  noise level is approximately  $60 \text{ MJy beam}^{-1}$ , and we detect a point source in the red map with a flux of 0.38 Jy and a point source with a flux of 0.36 Jy in the blue map. The centers of the point sources are separated by  $1''.9$ , with the red lobe to the west and the blue lobe to the east of the position of the H II region, as shown at the bottom of Figure 3.

### 4. CONCLUSION AND SUMMARY

The release of material from the surfaces of evolved intermediate-mass stars is an important ingredient in



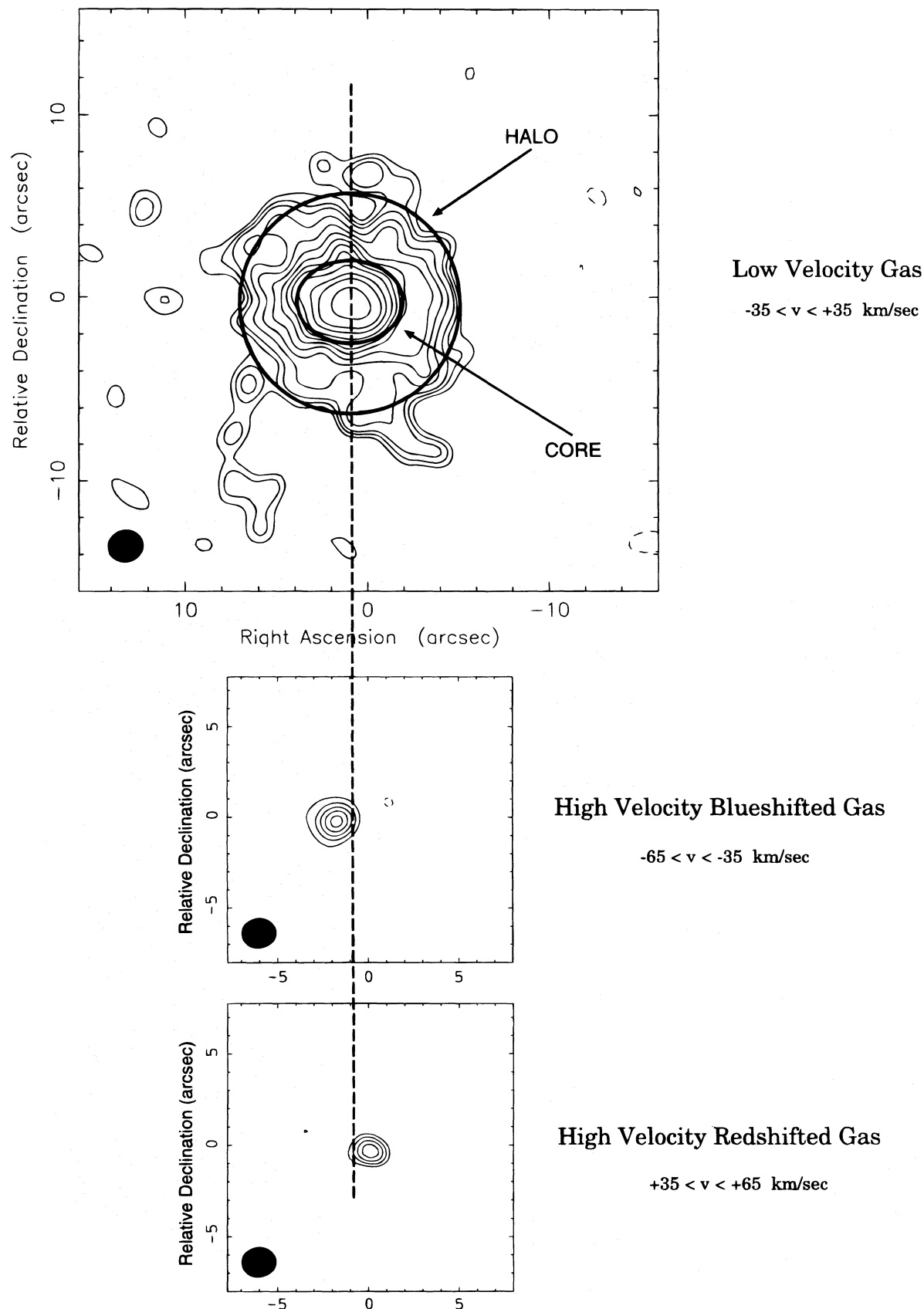


FIG. 3.—Total CO(1–0) line emission from CRL 618. The top plot shows the emission integrated from  $-35 < v < +35$  km s<sup>−1</sup>, which has two dominating morphological components: a spherical halo and a mildly bipolar (axial ratio = 0.76) core. The  $2\sigma$  noise level in this map is 33 mJy beam<sup>−1</sup>, and the contours are at the  $-3, 3, 4, 5, 7, 9, 11, 13, 15, 17, 20, 25, 30, 40, 50$ , and  $60\sigma$  levels. The lower two plots show the integrated high-velocity emission between  $+35 < v < +65$  km s<sup>−1</sup> for the redshift map and between  $-35 > v > -65$  km s<sup>−1</sup> for the blueshift map. The peak fluxes in these maps are 0.38 Jy and 0.36 Jy for the redshifted and blueshifted high-velocity maps, respectively, and the  $2\sigma$  noise level in these maps is 60 mJy beam<sup>−1</sup>. The centers of the point sources lie on opposite sides of the central source and are separated from each other by 1″9, providing clear evidence for the high-velocity bipolar jet in the core of CRL 618.

understanding the evolution of these stars. Since prodigious mass loss is a process experienced by stars throughout their asymptotic giant branch (AGB) evolution, envelope ejections will shape the morphology of future mass-loss episodes (Frank & Mellema 1994a, 1994b) and represent a significant fraction of the total stellar mass. Thus, such envelope ejections are critical in computing AGB evolution (Schonberner 1983; Wood & Faulkner 1986). Some observations of AGB stars have directly revealed the presence of circumstellar shells around the central stars (Waters et al. 1994; Young et al. 1993; Hawkins 1990; Gillett et al. 1986). But obtaining a reliable distance to the AGB star and the expansion velocity of the envelope are difficult to do directly, and the resulting mass and dynamical age computations are suspect. Some shells have been observed in the CO(1–0) transition, where at least the envelope velocity is readily available from the spectral line profile (Olofsson et al. 1992; Bujarrabal & Cernicharo 1994).

The suggestive appearance of dual concentric halos around the central star of CRL 618 has its analogs in the more developed and mature planetary nebulae (PNs). Even from the 1918 pioneering work of Curtis (1918), it was known that some PNs (Terzian 1983; Chu 1987). Observational estimates indicate that more than 50% of all PNs pass through the visible multiple-shell phase during their lifetime. A compilation of multiple-shell PNs by Chu, Jacoby, & Arendt (1987) includes 41 cases. Two types of structures are primarily seen; one has an inner shell expanding supersonically into a faint, subsonically expanding halo, and in the second has a bright outer envelope coexpanding with the inner shell. Some nebulae exhibit giant outer halos like NGC 6543 and NGC 6826, and a few PNs show triple shells like NGC 2022 and NGC 7662 (Chu et al. 1987; Middlemass et al. 1991; Middlemass, Clegg, & Walsh 1989). It is possible that CRL 618 will follow one of these paths. Already two major outflow events have been directly imaged in our CO maps in this paper in addition to the core and core outflow imaged in Hajian et al. (1995), Neri et al. (1992), and Martin-Pintado et al. (1995). If the blueshifted absorption feature in our maps is composed of two components, then each of these may represent absorption by cold matter in the other halo structures. Such a probe would best be attempted by very high resolution spectroscopic observations, with high dynamic range of the absorption feature corresponding to any emission line with a P Cygni feature.

Regardless of these speculations, it is likely that the structure we have imaged in CO is a bipolar core outflow expanding into a medium occupied by the remnant of a previously ejected shell (see Kwok 1987). The mass loss from the central star is also not smooth, as evidenced by the E–W collimation of the high-velocity outflow. At this point, the nature and origin of the blobs and plumes in the CO halo of CRL 618 are unclear, although several possibilities exist, each of which offers its own insights into the mass loss history of the central star. It is possible that the clumpy environment is shaped by holes in a preexisting density distribution generated by the wind from the progenitor red giant star. Regions of low CO opacity in a putative giant

halo would cause the portions of the halo directly behind it to be preferentially disassociated by the interstellar UV field. Thus, the knots may be regions of CO that are slow to dissociate, and to retain much of their initial CO density. Another possibility exists. If the outflow responsible for the giant halo terminated a significant time (with respect to the dynamical timescale of the halo) before the material comprising the CO halo was ejected from the stellar surface, then a cavity would have been excavated with which the CO halo and core outflows would expand. The blobs can be explained by a jet of material slamming into the walls of such a cavity and then generating instabilities (perhaps vortices) as the gas backflows with the inner boundary (B. Balick 1995, private communication). Finally, we suggest still another possibility. There have been numerous examples of planetary nebulae exhibiting FLIERs (Balick et al. 1993, 1994). FLIERs are small ( $\sim 1''$ ) localized regions that are usually found in pairs along the major axis of the nebula and are equidistant from and on opposite sides of the central star. They emit spectral lines from species that have a much lower ionization level than the adjacent gas. This is what might be expected if FLIERs represented a density enhancement in the nebular shell, but no enhancement is observed. Although no major axis is yet apparent in CRL 618, perhaps due to the youth of the nebula, it is possible that the knots in the CO halo we have detected are nascent FLIERs.

We would like to point out that no coherent model exists that couples the molecular observations to the ionized outflow and wind from the B0–O9.5 (Westbrook et al. 1975) central star. The ionized wind is likely fast and very tenuous, and the pressure-driven bubble it creates may affect the dynamics and appearance of any cool molecular gas it impacts. Currently, it is thought that the ionized outflow is the driving force behind the high-velocity molecular outflow, but this conclusion is more of a plausibility argument based on the pointlike and coincident appearance of both outflows and their high speeds. We hope that more progress will be made in the future in coupling these important components. With the sensitivity and high-angular resolution of the OVRO array, it would also be useful to search CRL 618 for structures analogous to the CO(1–0) halo, but in other molecules and/or CO transitions. Furthermore, given the prevalence of OR-emitting dust shells associated with molecular shells, it would be useful to image CRL 618 with ISO in order to learn more about the extended dust component of the circumstellar nebula while it is forming.

We would like to thank B. Balick for many profitable and illuminating discussions regarding the nature of the results. We also wish to extend our thanks to J. A. Cliffe for her constructive comments and her help with the figures. A. R. H. and Y. T. were supported in part by the National Astronomy and Ionosphere Center, which is operated by Cornell University under a cooperative agreement with the National Science Foundation. The OVRO millimeter interferometer is supported by NSF grant AST 90-16404.

#### REFERENCES

- Bachiller, R., Gomez-Gonzalez, J., Bujarrabal, V., Martin-Pintado, J. 1988, *A&A*, 196, L5  
 Balick, B., Perinotto, M., Maccioni, A., Terian, Y., & Hajian, A. R. 1993, *ApJ*, 424, 800  
 Balick, B., Rugers, M., Terzian, Y., & Chengalur, J. N. 1993, *ApJ*, 411, 778  
 Bujarrabal, V., & Cernicharo, J. 1994, *A&A*, 288, 551  
 Bujarrabal, V., Gomez-Gonzalez, J., Bachiller, R., & Martin-Pintado, J. 1988, *A&A*, 204, 242

- Cernicharo, J., Guelin, M., Martin-Pintado, J., Penálver, J., & Mauersberger, R. 1989, *A&A*, 22, L1
- Chu, Y. H. 1987, in *IAU Symp. 131, Planetary Nebulae*, ed. S. Torres-Piembert (Dordrecht: Kluwer), 105
- Chu, Y. H., Jacoby, G. H., & Arendt, R. 1987, *ApJS*, 64, 529
- Curtis, H. D. 1918, *Publ. Lick Obs.*, 13, 57
- Deguchi, S., Claussen, M. J., & Goldsmith, P. F. 1986, *ApJ*, 303, 810
- Frank, A., & Mellema, G. 1994a, *ApJ*, 430, 800
- . 1994b, *A&A*, 289, 937
- Gammie, C. F., Knapp, G. R., Young, K., Phillips, T. G., & Falgarone, E. 1989, *ApJ*, 345, L87
- Gillett, F. C., Backman, D. E., Beichman, C., & Neugebauer, G. 1986, *ApJ*, 310, 842
- Gottlieb, E. W., & Liller, W. 1976, *ApJ*, 207, L135
- Hajian, A. R., Phillips, J. A., & Terzian, Y. 1995, *ApJ*, 446, 244
- Hawkins, G. W. 1990, *A&A*, 229, L5
- Kawabe, R., et al. 1989, *ApJ*, 314, 322
- Kelly, D. M., Latter, W. B., & Rieke, G. H. 1992, *ApJ*, 395, 174
- Kwok, S. 1987, in *Late Stages of Stellar Evolution*, ed. S. Kwok & S. R. Pottasch (Dordrecht: Reidel), 321
- Kwok, S., & Bignell, R. C. 1984, *ApJ*, 276, 544
- Kwok, S., & Feldman, P. A. 1981, *ApJ*, 247, L67
- Kwok, S., Hrivnak, B. J., & Milone, E. F. 1986, *ApJ*, 303, 451
- Lo, K. Y., & Bechis, K. P. 1976, *ApJ*, 205, L21
- Martin-Pintado, J., & Bachiller, R. 1992, *ApJ*, 391, L93
- Martin-Pintado, J., Gaume, R. A., Johnson, K. J., & Bachiller, R. 1995, *ApJ*, 446, 687
- Middlemass, D., Clegg, R. E. S., & Walsh, J. R. 1989, *MNRAS*, 239, 1
- Middlemass, D., Clegg, R. E. S., Walsh, J. R., & Harrington, J. P. 1991, *MNRAS*, 251, 284
- Neri, R., Garcia-Burillo, S., Guelin, M., Cernicharo, J., Guilloteau, S., & Lucas, R. 1992, *A&A*, 262, 544
- Olofsson, H., Carlstrom, U., Eriksson, K., & Gustafsson, B. 1992, *A&A*, 253, L17
- Padin, S., et al. 1993, *IEEE Trans. Instrum. Meas.*, 42, 793
- Schmidt, G. D., & Cohen, M. 1981, *ApJ*, 246, 444
- Schonberger, D. 1983, *ApJ*, 272, 708
- Scoville, N. Z., Carlstrom, J. E., Chandler, C. J., Phillips, J. A., Scott, S. L., Tilanus, R. P. J., & Wang, Z. 1993, *PASP*, 105, 1482
- Schibata, K. M., Deguchi, S., Hirano, N., Kameya, O., & Tamura, S. 1993, *ApJ*, 415, 708
- Sopka, R. J., Hildebrand, R., Jaffe, D. T., Gatley, I., Roellig, T., Werner, M., Jura, M., & Zuckerman, B. 1995, *ApJ*, 2994, 242
- Terzian, Y. 1983, in *IAU Symp. 103, Planetary Nebulae*, ed. D. R. Flower (Dordrecht: Reidel), 487
- Trammell, S. R., Dinerstein, H. L., & Goodrich, R. W. 1993, *ApJ*, 402, 249
- Waters, L. B. F. M., Loup, C., Kester, D. J. M., Bontekoe, Tj. R., & de Jong, T. 1994, *A&A*, 281, L1
- Westbrook, W. E., Becklin, E. E., Merrill, K. M., Neugebauer, G., Schmidt, M., Willner, S. P., & Wynn-Williams, C. G. 1975, *ApJ*, 202, 407
- Wood, P. R., & Faulkner, D. J. 1986, *ApJ*, 307, 659
- Yamamura, I., Shibata, K. M., Kasuga, T., & Deguchi, S. 1994, *ApJ*, 427, 406
- Young, K., Phillips, T. G., & Knapp, G. R. 1993, *ApJ*, 409, 725
- Young, K., Serabyn, G., Phillips, T. G., Knapp, G. R., Gusten, R., & Schulz, A. 1992, *ApJ*, 385, 265